The antidiabetic drug troglitazone protects against PrP (106-126)-induced neurotoxicity via the PPARγ-autophagy pathway in neuronal cells

JI-HONG MOON, JEONG-MIN HONG and SANG-YOUEL PARK

Biosafety Research Institute, College of Veterinary Medicine, Jeonbuk National University, Iksan, Jeonbuk 54596, Republic of Korea

Received September 4, 2020; Accepted March 16, 2021

DOI: 10.3892/mmr.2021.12069

Abstract. Prion diseases, which involve the alteration of cellular prion protein into a misfolded isoform, disrupt the central nervous systems of humans and animals alike. Prior research has suggested that peroxisome proliferator-activator receptor (PPAR)γ and autophagy provide some protection against neurodegeneration. PPARs are critical to lipid metabolism regulation and autophagy is one of the main cellular mechanisms by which cell function and homeostasis is maintained. The present study examined the effect of troglitazone, a PPARγ agonist, on autophagy flux in a prion peptide (PrP) (106-126)-mediated neurodegeneration model. Western blot analysis confirmed that treatment with troglitazone increased LC3-II and p62 protein expression, whereas an excessive increase in autophagosomes was verified by transmission electron microscopy. Troglitazone weakened PrP (106-126)-mediated neurotoxicity via PPARγ activation and autophagy flux inhibition. A PPARγ antagonist blocked PPARγ activation as well as the neuroprotective effects induced by troglitazone treatment, indicating that PPARγ deactivation impaired troglitazone-mediated protective effects. In conclusion, the present study demonstrated that troglitazone protected primary neuronal cells against PrP (106-126)-induced neuronal cell death by inhibiting autophagic flux and activating PPARγ signals. These results suggested that troglitazone may be a useful therapeutic agent for the treatment of neurodegenerative disorders and prion diseases.

Introduction

Transmissible spongiform encephalopathies (TSEs) are fatal neurodegenerative diseases caused by prions (1). TSEs have common pathognomonic and histopathological characteristics, including spongiform changes, glial proliferation, neuronal loss, and the deposition of a misfolded isoform (PrPsc) (2) of the cellular prion protein (PrPc). Whether the prion disease at issue is genetic, transmissible, or an irregular disorder, they all implicate protein refolding of the normal prion (PrPc), which is encoded by the *Prnp* gene (3). PrPsc, a misfolded version of PrPc, was originally thought to be an accumulated proteinase K-resistant prion protein. However, patients with PrPc could still incur disease-related and diagnostically imperative alterations even without its conversion to the protease-resistant form (4).

Synthetic human prion peptide (PrP) (106-126) preserves some features of PrPsc's physiological and pathogenic assets and can initiate apoptosis of hippocampal neurons (5). An investigation of the respective amino acid sectors showed that the peptide, including amino acids 106-126 of the PrP sequence, was able to replicate several biological features of PrPsc *in vitro*, including amyloidogenesis, as well as its neurotoxic and its gliotrophic effects (6-8). Moreover, PrP (106-126) covers an AGAAAAGA arrangement at amino acids 113 to 120, a motif that has been found in PrP molecules across numerous species (9).

Troglitazone is an antidiabetic medicine used to treat type 2 diabetes, improve the sensitivity of various tissues to insulin, and reduce blood glucose levels (10-12). Troglitazone's antidiabetic effects are closely related to peroxisome proliferator-activated receptor (PPAR)γ activation, which suggests that it is the activation of PPAR-responsive genes that is responsible for the insulin-sensitizing effects of troglitazone (13-15). PPARγ is a member of the class of PPARs that are associated with ligand-stimulated nuclear receptors (16). PPARγ is primarily expressed in adipose tissue and plays an important role in lipid metabolism alteration, insulin sensitivity, and adipocyte differentiation (17,18). Some studies have proposed that PPARγ activation has a protective effect on neuronal cells and inhibits neurodegeneration (19-22). With this in mind, we investigated whether troglitazone protected against prion peptide-mediated neuronal apoptosis.

Autophagy, also known as programmed cell death-II, is a homeostatic and catabolic progression by which cellular constituents and organelles are delivered to lysosomes for degradation (23,24). Autophagy begins with the development

Correspondence to: Professor Sang-Youel Park, Biosafety Research Institute, College of Veterinary Medicine, Jeonbuk National University, 79 Gobong-ro, Iksan, Jeonbuk 54596, Republic of Korea
E-mail: sypark@chonbuk.ac.kr

Key words: troglitazone, prion protein, autophagy flux, PPARγ, neurotoxicity

of double-membrane structures (autophagosomes) that enclose cellular ingredients and organelles. Once these are combined with lysosomes, they progress to a maturing system and, ultimately resulting in the collapse and recycling of the cargo (25,26). p62 levels correlate with autophagy (27). While p62 is selectively degraded by autolysosomal degradation, it is not degraded by the ubiquitin-proteasome system (UPS) (28). p62 levels increase when autophagy is repressed (29,30).

In our prior research, we uncovered that the inhibition of autophagy prevented PrP (106-126)-mediated neuronal cytotoxicity (31). In this study, we investigate whether troglitazone protects against PrP (106-126)-mediated neuronal cytotoxicity via autophagy flux and whether the autophagy flux is controlled by PPARγ.

Materials and methods

Cell culture. Embryonic 18-day ICR mice were purchased from SAMTAKO (Osan, Korea). No experiments were performed on live animals. The animals were euthanized by cervical dislocation and the brain was collected from the pups. Primary murine cortex neuron culture was performed according to the protocol of Beaudoin *et al* (32) and a little modified. Brain was dissected in Hanks Buffered Saline Solution without Mg^{2+} and Ca^{2+} (HBSS: Gibco; Thermo Fisher Scientific, Inc.) and digested in 0.25% trypsin containing DNAse I (2,000 U/mg) (Gibco; Thermo Fisher Scientific, Inc.) for 20 min at 37˚C. The obtained cell suspension was diluted in DMEM containing 25 mM glucose and 10% fetal bovine serum (FBS), and then cultured in tissue culture flasks coated with 50 μg/ml poly-D-lysine at a density of 3-4x10^5 cells/cm^2. The SK-N-SH (human neuroblastoma cell line, passage no. 14) was acquired from the American Type Culture Collection (ATCC). SK-N-SH cells were cultured in Minimum Essential Medium (Hyclone Laboratories) with 10% fetal bovine serum (FBS, Gibco; Thermo Fisher Scientific, Inc.) and gentamycin (0.1 mg/ml) at 37˚C and 5% CO_2.

Chemical and PrP (106-126) treatment. Synthetic prion peptides PrP (106-126) (Lys-Thr-Asn-Met-Lys-His-Met-Ala-Gly-Ala-Ala-Ala-Ala-Gly-Ala-Val-Val-Gly-Gly-Leu-Gly) were manufactured by Peptron. The peptides were dissolved in sterile dimethyl sulfoxide (DMSO) at a stock concentration of 10 mM and stored at -20˚C.

The stock solution of troglitazone (8 mM; Sigma-Aldrich; Merck KGaA) was dissolved in DMSO. The cells were pre-incubated with 20, 40, or 80 μM troglitazone with/without PrP (100 μM) for 12 h. For the inhibitor treatments, the cultures were pretreated with a 10 μM CQ (autophagy inhibitor; Sigma-Aldrich) or 10 μM GW9662 (PPARγ antagonist; Sigma-Aldrich; Merck KGaA).

Trypan blue exclusion assay. Cell viability was evaluated by trypan blue exclusion assay using a hemocytometer. Untreated cells were used as the control group and cell viability was compared with the control. Each treatment was performed in triplicate.

Annexin V/PI assay. Cells in the logarithmic phase were collected and cultured in 24-well plates at 4x10^4 cells/well. Cell survival was evaluated using an Annexin V/PI Assay Kit (Santa Cruz Biotechnology) following the manufacturer's procedure. Briefly, cells were treated for 24 h and then harvested, washed in cold phosphate-buffered saline (PBS) twice and then stained with fluorescein isothiocyanate (FITC)-conjugated Annexin V and PI dyes. The externalization of phosphatidylserine and the permeability to PI were evaluated using a flow cytometer. Data from 5,000 gated events per sample were collected. Cells in early stages of apoptosis were positively stained with Annexin V, whereas cells in late apoptosis were positively stained with both Annexin V and PI. The fluorescence was determined at 488 nm excitation and 525/30 emission using a Guava EasyCyte HT System (Millipore).

Terminal deoxynucleotidyl transferase dUTP nick end-labeling (TUNEL) assay. Cells in the logarithmic phase were collected and cultured in 6-well plates at 3x10^5 cells/well. Neuronal apoptosis was assessed after treatment using an ApoBrdU DNA Fragmentation Assay Kit (BioVision), following the manufacturer's instructions. The nuclei were counterstained with PI.

RNA interference. SK-N-SH cells were transfected with ATG5 small-interfering RNA (siRNA; oligoID HSS114104; Invitrogen; Thermo Fisher Scientific, Inc.) using Lipofectamine 2000 according to the manufacturer's instructions. After a 48-h culture, knockdown efficiency was measured at the protein level by immunoblot analysis. Nonspecific siRNA (oligoID 12935-300; Invitrogen; Thermo Fisher Scientific, Inc.) was used as the negative control.

BacMam transduction. GFP-LC3B puncta assay was evaluated in neuronal cells using the virus from the Premo Autophagy Sensor LC3B-GFP (BacMam 2.0) kit (Life Technologies, P36235). LC3B-FP and LC3B (G120A)-FP viral vectors (MOI, 30) were employed to monitor autophagosome dynamics by fluorescence microscopy analysis.

Immunocytochemistry. Cells in the logarithmic phase were collected and cultured on 1% gelatin-coated coverslips (12 mm; Nalge Nunc International) in 24-well plates at 4x10^4 cells/well. After treatment, the cells were fixed with 4% PFA in PBS (1X) at pH 7.4 for 20 min at room temperature (RT). The cells were washed in sterile Tris-buffered saline TBS (1M), 3 g Tris (24.8 mM), 8 g NaCl (137 mM), and 0.2 g KCl (2.7 mM) in 1 liter distilled water at pH 7.4 with 0.1% Tween-20 (TBST) for 10 min. They were then blocked for 15 min in TBST with 5% FBS, and incubated for 3 h at RT with the primary antibodies (anti-PPARγ diluted 1:1,000; sc-7273; Santa Cruz Biotechnology), which had themselves been diluted in TBST with 5% FBS. Alexa Fluor 488-labeled donkey anti-rabbit IgG antibody (A21206; Molecular Probes) diluted 1:1,000 was employed to visualize the channel expression using fluorescence microscopy (Nikon Eclipse 80i). The images were evaluated using NIS-Elements F Ver4.60 imaging software.

Confocal microscopy. After being subjected to either immunocytochemistry or the GFP-LC3B puncta assay, the coverslips were placed in mounting medium and imaged through a 63x

oil objective on a Zeiss LSM710 microscope equipped with a standard set of lasers. The excitation wavelengths were 488, 543, and 633 nm. The bandpass filters were set at 500-550 (AlexaFluor488), 560-615 nm (Cy3, AlexaFluor568), and 650-750 nm (AlexaFluor647).

Western blot analysis. Cells in the logarithmic phase were collected and cultured in 6-well plates at $3x10^5$ cells/well. After the treatments, the cells were washed with PBS and lysed in lysis buffer [25 mM HEPES (4-(2-hydroxyethyl)-1-piperazineethanesulfonic acid) at pH 7.4, 100 mM NaCl, 1 mM ethylenediaminetetraacetic acid (EDTA), 5 mM $MgCl_2$, 0.1 mM dithiothreitol (DTT), and a protease inhibitor mixture]. Equal quantities of cellular proteins (15-30 μg/μl) were electrophoretically resolved on a 10% sodium dodecyl sulfate (SDS) polyacrylamide gel and transferred to a nitrocellulose membrane. Immunoreactivity was detected through consecutive incubations with a blocking solution containing 5% skim milk and primary antibodies followed by the corresponding horseradish peroxidase-conjugated secondary antibodies, and finally developed using enhanced chemiluminescence substances in the WESTSAVE Gold Detection Kit (LF-QC0103; AbFrontier Inc.). The primary antibodies, anti-PPARγ diluted 1:1,000 (sc-7273; Santa Cruz Biotechnology), anti-LC3B diluted 1:1,000 (#4108; Cell Signaling Technology), anti-P62 diluted 1:1,000 (#5114; Cell Signaling Technology) and anti-β-actin diluted 1:5,000 (A5441; Sigma-Aldrich; Merck KGaA), in the antibody solution (1% skim milk in TBST) were used for immunoblotting. The images were inspected using a Fusion FX7 imaging system (Vilber Lourmat, Torcy Z.I. Sud). The density of the signal bands was evaluated using Bio-1D software (Vilber Lourmat).

Transmission electron microscopy (TEM) analysis. The cells for TEM were fixed in 2% glutaraldehyde [Electron Microscopy Sciences (EMS)] and 2% paraformaldehyde (EMS) in 0.05 M sodium cacodylate (pH 7.2; EMS) for 2 h at 4˚C. The samples were fixed in 1% osmium tetroxide (EMS) for 1 h at 4˚C, dehydrated with a graded ethanol series (25, 50, 70, 90 and 100%) for 5 min each, and embedded in epoxy resin (Embed 812; EMS) for 48 h at 60˚C following to the manufacturer's instructions. Ultrathin sections (60 nm) were cut using an LKB-III Ultratome (Leica Microsystems GmbH) and stained with 0.5% uranyl acetate (EMS) for 20 min and 0.1% lead citrate (EMS) for 7 min at RT. The fluorescent images were recorded on a Hitachi H7650 electron microscope (Hitachi, Ltd.; magnification, x10,000) installed at the Center for University-Wide Research Facilities (CURF) at Jeonbuk National University.

Statistical analysis. Results are expressed as the means ± standard deviations (SD) from at least three independent replicates. All experiments were analyzed by the one-way analysis of variance. Comparisons of three or more groups were made using Tukey's post hoc test. All statistical analyses were implemented with GraphPad Prism version 5.0 software. $P<0.05$ was considered to indicate a statistically significant difference.

Results

Protective effect of troglitazone on prion protein-mediated neuronal cell death. Consistent with the relevant literature (33,34) and our preliminary experiments, we used different concentrations of troglitazone for efficacy testing. We selected 80 μM troglitazone as highest concentration because it significantly increased cell viability (at 100 μM PrP). Once our preliminary experiments were complete, we proceeded to examine the effect of troglitazone on PrP (106-126)-mediated neurotoxicity by an Annexin V/PI assay in primary neuronal cells. Cells were treated with PrP in combination with troglitazone. PrP treatment led to a 2.25-fold decrease in cell viability (Annexin V^-/PI^-) compared to the control. In detail, PrP treatment increased early apoptosis (Annexin V^+/PI^-) from about 2% to about 30% and late apoptosis (Annexin V^+/PI^+) from about 1% to about 19%. We observed that pretreatment with troglitazone dose-dependently protected neurons against PrP (106-126)-induced neurotoxicity. Treatment of the cells with 20, 40, and 80 μM troglitazone increased cell viability by 1.18±1.20 (SD), 1.34±1.19 (SD), and 1.70±1.23 (SD)-fold, respectively, compared to PrP-treated cells (Fig. 1A and B). In addition, we confirmed the protective effect of 80 μM troglitazone in SK-N-SH cells (data not shown). Consistent with this, in the trypan blue assay, troglitazone repressed PrP-mediated cell death dose-dependently (Fig. 1C). Troglitazone also decreased DNA strand damage triggered by PrP treatment (Fig. 1D and E). These results indicate that troglitazone attenuated PrP (106-126)-mediated neuronal cell death.

Troglitazone restrains autophagy flux in neuronal cells. It has traditionally been thought that LC3 and SQSTM1/p62 are consumed by lysosomal degradation via the process of autophagy flux (28). We found that LC3-II and SQSTM1/p62 protein levels were increased in the troglitazone-treated groups. Treatment of the cells with 80 μM troglitazone increased SQSTM1/p62 protein level by 2.44±0.50-fold compared to the control (Fig. 2A and B). The BacMam 2.0 system was employed to observe the construction of autophagosomes in the neuroblastoma cells. Troglitazone led to an increase in punctate fluorescence in SK-N-SH cells (Fig. 2C and D). The observed punctate fluorescence distribution pattern suggested that the LC3B-FP protein was collected in the autophagosomes. Using transmission electron microscopy (TEM), we observed that troglitazone treatment improved phagophore accumulation that was not degraded by the lysosomes (Fig. 2E and F), suggesting that troglitazone inhibited autophagy flux in neuronal cells. To demonstrate the effect of autophagy inhibition on PrP-mediated neuronal cell death, we performed cell viability assays using Annexin V/propidium iodide (PI) with/without chloroquine (CQ). We chose the CQ concentration on the basis of other studies (35,36). We confirmed that, like the CQ autophagy inhibitor, troglitazone had neuroprotective effects via autophagy inhibition (Fig. 3A and B). We also found that troglitazone and CQ increased levels of p62 and LC3B-II protein (Fig. 3C and D), suggesting an inhibition of autophagy flux. On the basis of the observation that p62 protein level and cell viability did not increase by more when troglitazone and CQ were treated together, we propose that troglitazone and CQ play the same role in inhibiting autophagy flux.

Moreover, the Atg5 knockdown had little impact on troglitazone-mediated neuroprotection (Fig. 4A and B) and inhibition of autophagy flux (Fig. 4C and D). Specifically, troglitazone repressed autophagy flux and PrP-mediated neuronal apoptosis

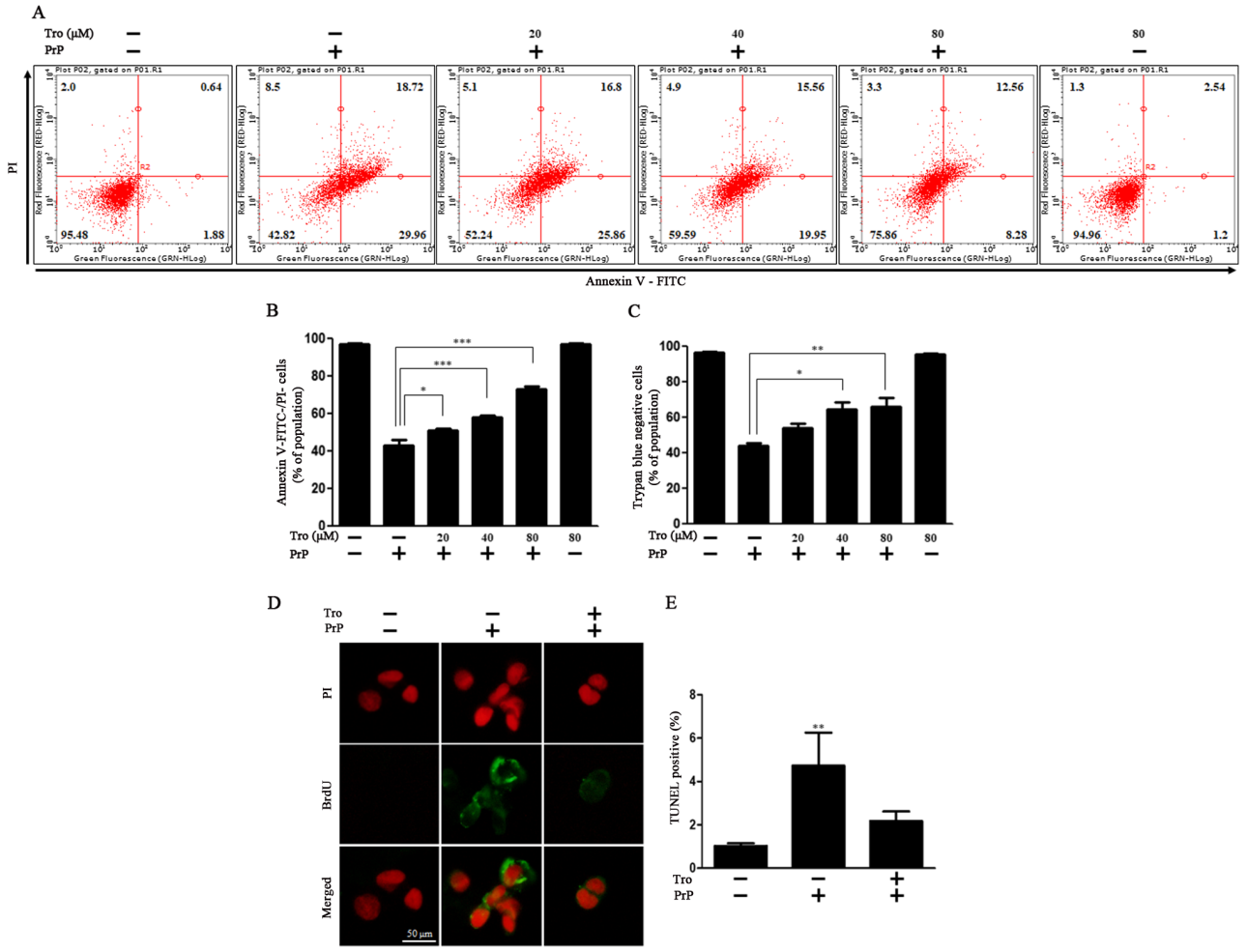

Figure 1. Troglitazone decreased PrP (106-126)-induced neuronal cell death. (A) Primary neurons were pretreated with troglitazone (1 h) in a dose-dependent manner and then exposed to 100 μM PrP (106-126) for 12 h. Cell viability was evaluated by an Annexin V/PI assay using FITC-Annexin V, which combined with phosphatidylserine on the plasma membrane during the apoptotic processes. Representative figures showing population of viable (Annexin V^-/PI^-), early apoptotic (Annexin V^+/PI^-), late apoptotic (Annexin V^+/PI^+) and necrotic (Annexin V^-/PI^+) cells. (B) Bar graph showing the averages of viable (Annexin V^-/PI^-) cells. Values represent the mean ± SD (n=10). $^*P<0.05$, $^{***}P<0.001$. (C) Cell viability was measured by a trypan blue dye exclusion assay in primary neuron cells. Values represent the mean ± SD (n=5). $^*P<0.05$, $^{**}P<0.01$. (D) TUNEL-positive (green) immunofluorescence images were obtained after exposure to 100 μM PrP (106-126) (12 h) in the absence or presence of troglitazone (1 h). The cell nuclei were counterstained with PI (red). (E) Values represent the mean ± SD (n=5). $^{**}P<0.01$ vs. untreated cells. PrP, prion peptide (106-126); Tro, troglitazone.

by inhibiting fusion between the autophagosome and the lysosome, not by reduction of Atg5. We confirmed the successful siRNA transfection of ATG5 through additional experiments; the results revealed that Atg5 siRNA reduced the expression levels of Atg5 and LC3B, and increased p62 (Fig. S1). These experimental results indicate that troglitazone or Atg5 knockdown result in an inhibition of autophagy flux, and thereby exert a neuroprotective effect in an *in vitro* prion model.

PPARγ activation by troglitazone attenuates PrP (106-126)-mediated neuronal cell death via inhibition of autophagy flux. We evaluated whether troglitazone-activated PPARγ weakened prion peptide-mediated neuronal cell death by inhibiting autophagy flux. Troglitazone dose-dependently increased the activation of PPARγ, as indicated by the red fluorescence in Fig. 5C and D. Treatment of the cells with 80 μM troglitazone increased PPARγ protein levels by 3.74±0.60-fold compared to the control (Fig. 5A and B). PPARγ antagonist GW9662, which was employed at a concentration consistent with previous studies (37,38), suppressed PPARγ activation. Moreover, increased LC3-II and p62 protein expression, which indicates the inhibition of autophagy flux, was reversed by the PPARγ antagonist (Fig. 6A and B). These experiments demonstrate that troglitazone-induced inhibition of autophagy flux is regulated by PPARγ. To investigate the effect of PPARγ activation on PrP-mediated neurotoxicity, we performed cell viability experiments with and without the PPARγ antagonist. We determined that troglitazone's neuroprotective effect was inhibited by the PPARγ antagonist (Fig. 6C and D). This data collectively provides a strong basis for our conclusion that PPARγ activation by troglitazone prevents PrP (106-126)-mediated neurotoxicity by inhibiting autophagy flux.

Discussion

The purpose of this study was to investigate whether troglitazone could be a potential agent for targeting PPARγ and autophagy flux, thereby decreasing prion protein-mediated neuronal cell death. Our findings confirm troglitazone's potential as a therapeutic agent in response to neurodegenerative diseases, including prion diseases. We suggest that the PPARγ

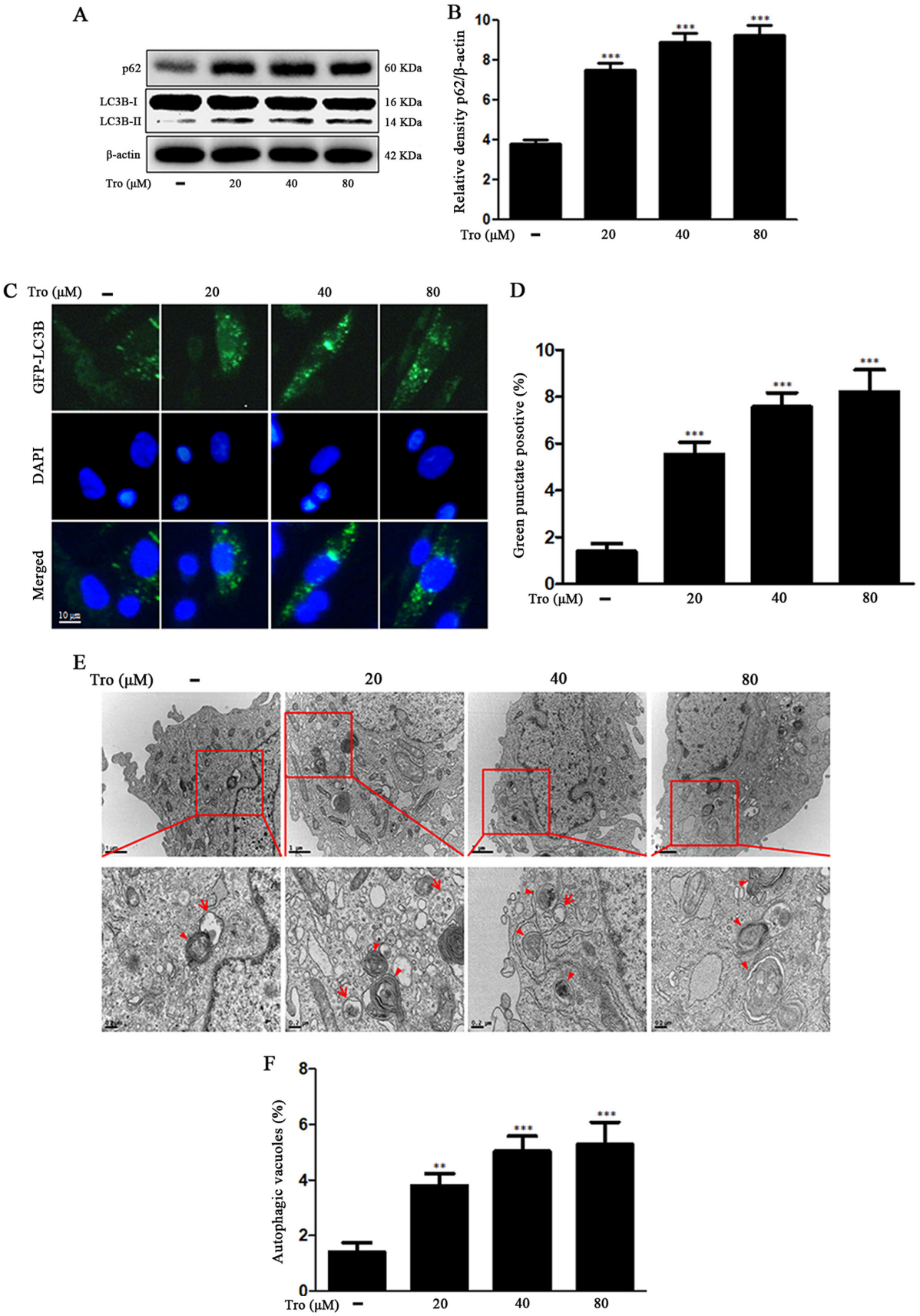

Figure 2. Troglitazone inhibited autophagic flux in neuronal cells. (A) Primary neuronal cells were treated with 20, 40, or 80 μM of troglitazone for 6 h. The treated cells were evaluated for LC3B and p62 expression by western blot analysis. (B) Bar graph representing average p62 protein levels. Expression data were normalized to β-actin expression. Expression levels were evaluated by quantifying the protein bands, depicted by densitometric values beside the blot. Values represent the mean ± SD (n=5). ***P<0.001 vs. control. (C) SK-N-SH cells were treated with a titration (30 MOI) of BacMam GFP-LC3B virus over 18 h and then treated with varying concentrations of troglitazone for 6 h. The cell nuclei were stained with DAPI (blue). (D) Values represent the mean ± SD (n=5). ***P<0.001 vs. control. (E) SK-N-SH cells were treated with 20, 40, or 80 μM troglitazone for 6 h and analyzed by TEM. Arrowheads designate autophagosomes and arrows indicate autolysosomes. (F) Values represent the mean ± SD (n=5). **P<0.01, ***P<0.001 vs. control. Tro, troglitazone.

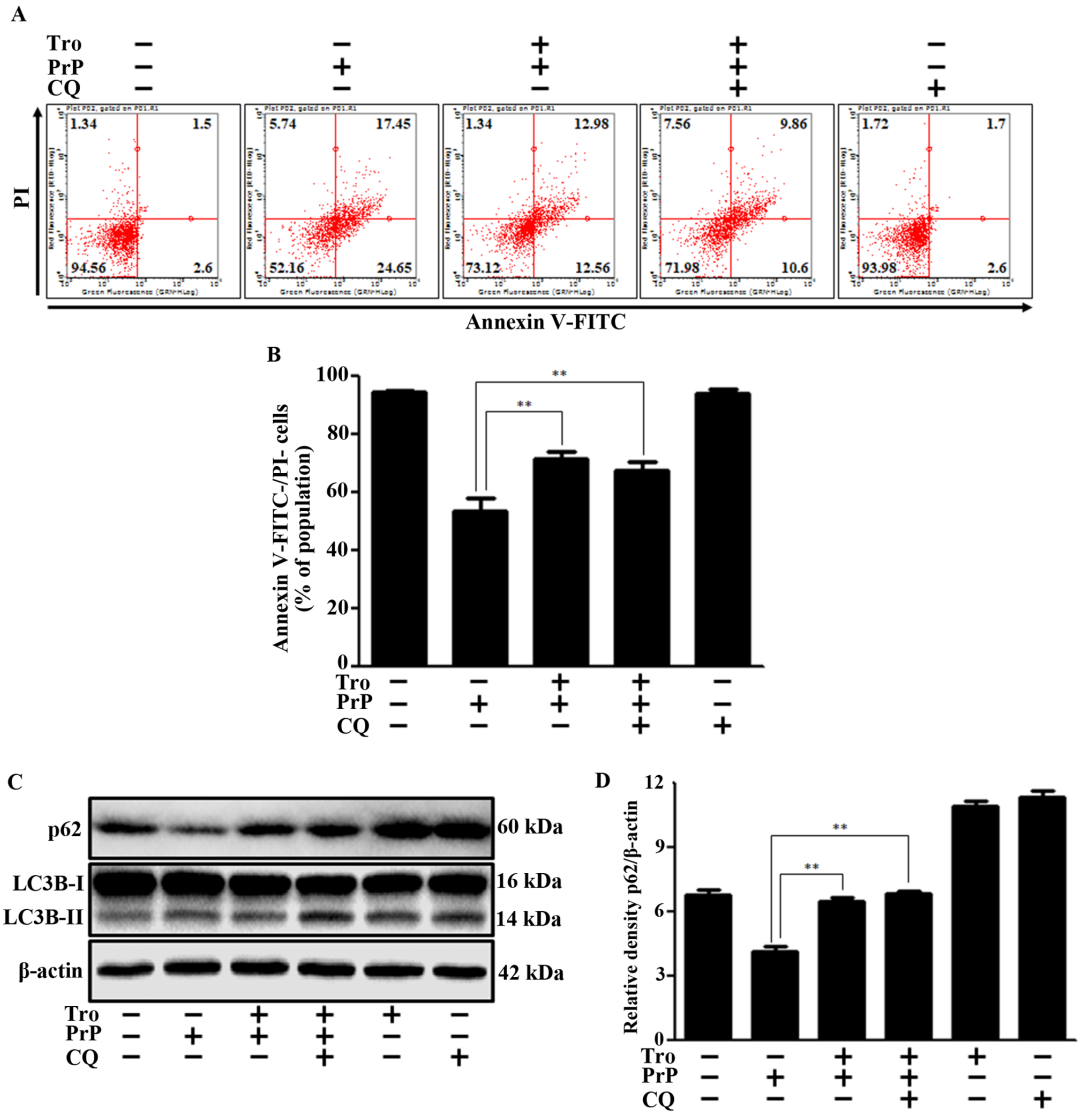

Figure 3. Troglitazone protected against PrP (106-126)-induced neuronal apoptosis by inhibiting autophagy flux. (A) SK-N-SH cells were pretreated with troglitazone (80 μM) or autophagy inhibitor (10 μM CQ) for 1 h and then exposed to 100 μM PrP (106-126) for 12 h. Cell viability was evaluated by an Annexin V/PI assay using FITC-Annexin V and PI, which combined with phosphatidylserine on the plasma membrane and nuclei during cellular apoptosis. Representative figures showing population of viable (Annexin V^-/PI^-), early apoptotic (Annexin V^+/PI^-), late apoptotic (Annexin V^+/PI^+) and necrotic (Annexin V^-/PI^+) cells. (B) Bar graph showing the averages of viable (Annexin V^-/PI^-) cells. Values represent the mean ± SD (n=10). **P<0.01. (C) Primary neuronal cells were pretreated with troglitazone or CQ (1 h) and then exposed to 100 μM PrP (106-126) for 6 h. LC3B and P62 expression was measured by western blot analysis. β-actin was applied as a loading control. (D) Bar graph representing average p62 protein levels. Expression data were normalized to β-actin expression. Expression levels were evaluated by quantifying the protein bands, depicted by densitometric values beside the blot. Values represent the mean ± SD (n=5). **P<0.01. PrP, prion peptide (106-126); Tro, troglitazone; CQ, chloroquine.

signaling and autophagy flux affected by troglitazone might be a strategic mechanism to target in prion disease.

Nah *et al* (39) reported that the *Prnp* gene activates autophagy in response to the presence of amyloid-β in neuronal cells. A number of studies have theorized that autophagy generates cellular apoptosis (40-43). These studies underlie our assumption that the amyloid plaque formed by PrPsc accumulates and stimulates neuronal autophagic cell death. In a previous study, we determined that human prion peptide 106-126 stimulated acute autophagy flux to promote autophagic cell death in neurons and that CQ attenuated PrP-induced neurotoxicity via autophagy inhibition (31). In this study, we determined that autophagy inhibition by troglitazone could protect neuronal cells against PrP-induced cell death. Troglitazone inhibited PrP-mediated autophagic cell death, and the addition of CQ had no change on the protective effect (Fig. 3). As co-treatment with troglitazone and CQ resulted in no synergic effect, that the inference to be drawn is that troglitazone inhibited autophagic signals. This result was further affirmed in our tests using Atg5 siRNA tools (Fig. 4).

We explored upstream of the troglitazone- induced neuronal autophagy flux. Troglitazone, a PPARγ agonist, suppresses the excretion of inflammatory cytokines and neurotoxic agents from stimulated monocytes and microglia, and thus has anti-inflammatory properties (44-46). We determined that troglitazone stimulated PPARγ activation, which in turn regulated PrP-mediated autophagic cell death.

The anti-inflammatory functions of PPARγ have recently received a great deal of attention, as its agonists have been

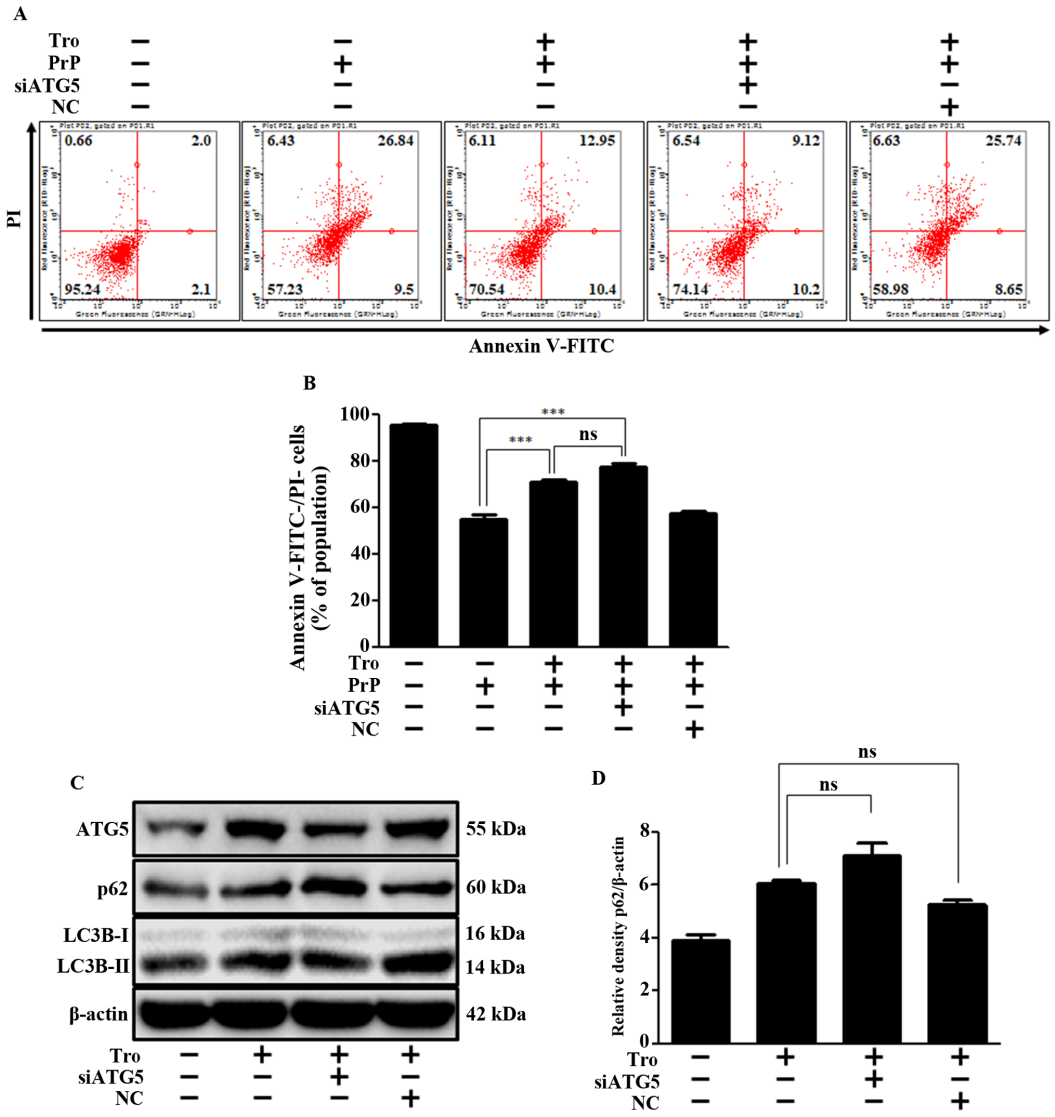

Figure 4. ATG5 knockdown did not influence the troglitazone-mediated neuroprotective effect. (A) siATG5 or NC-transfected cells (SK-N-SH) were exposed to PrP (106-126) for 12 h in the absence or presence of troglitazone. Cell viability was evaluated by the Annexin V/PI assay. Representative figures showing population of viable (Annexin V^-/PI^-), early apoptotic (Annexin V^+/PI^-), late apoptotic (Annexin V^+/PI^+) and necrotic (Annexin V^-/PI^+) cells. (B) Bar graph showing the averages of viable (Annexin V^-/PI^-) cells. Values represent the mean ± SD (n=10). $^{***}P<0.001$. (C) Western blot analysis for ATG5, p62, and LC3B protein expression in neuroblastoma cells (SK-N-SH). β-actin was applied as a loading control. (D) Bar graph representing the average p62 protein expression levels. Expression data were normalized to β-actin expression. Expression levels were evaluated by quantifying the protein bands, depicted by densitometric values beside the blot. Values represent the mean ± SD (n=5). PrP, prion peptide (106-126); Tro, troglitazone; NC, negative control; siATG5, ATG5 small-interfering RNA.

shown to exert protective effects in neurologic diseases (47-49). Some studies have reported that PPARγ ligands protect against the oxidative stress in neuronal injury (50-52), while others have suggested that PPARγ activation may obstruct autophagy flux (53-55). In this paper, we demonstrated that troglitazone activated PPARγ in neurons and used a PPARγ inhibitor to prevent PrP-mediated autophagic cell death (Figs. 5 and 6). These findings suggest that troglitazone-activated PPARγ protected neuronal cells against PrP-induced cell death via autophagy inhibition. Previous studies suggested several materials, such as resveratrol, could prevent prion-induced neurotoxicity (56,57). This is the first study indicating that troglitazone-mediated PPARγ may play a critical role in the neuroprotection against PrP (106-126)-induced neurotoxicity.

Similar to PrPsc, a neurotoxic prion protein segment, PrP (106-126), preserves biochemical substances, such as protease resistance, β-sheet formation, and cytotoxicity (6,58-60). Some studies have investigated prion pathogenesis and neurotoxic pathways *in vivo* using Rocky Mountain Laboratory (RML) infection and antibody-derived anti-PrP ligands (61-63). In these studies, the neurodegenerative changes typical of prion diseases were observed without detectable PrPsc, suggesting the presence of additional mechanisms of neuronal death in prion disorders, aside from those related to PrPsc (64,65). We suggest that prion peptide may have valuable role as a therapeutic strategy for prion diseases though PrP (106-126) is not equivalent to PrPsc. We found that the 106-126 sequence of the prion protein is an efficient model for *in vitro* study of prion-induced cell death, as it results in rapid depolarization of mitochondrial membranes. Based on these observations, it was suggested that PrP (106-126) is a major contributor to the physicochemical and pathogenic properties of PrPsc.

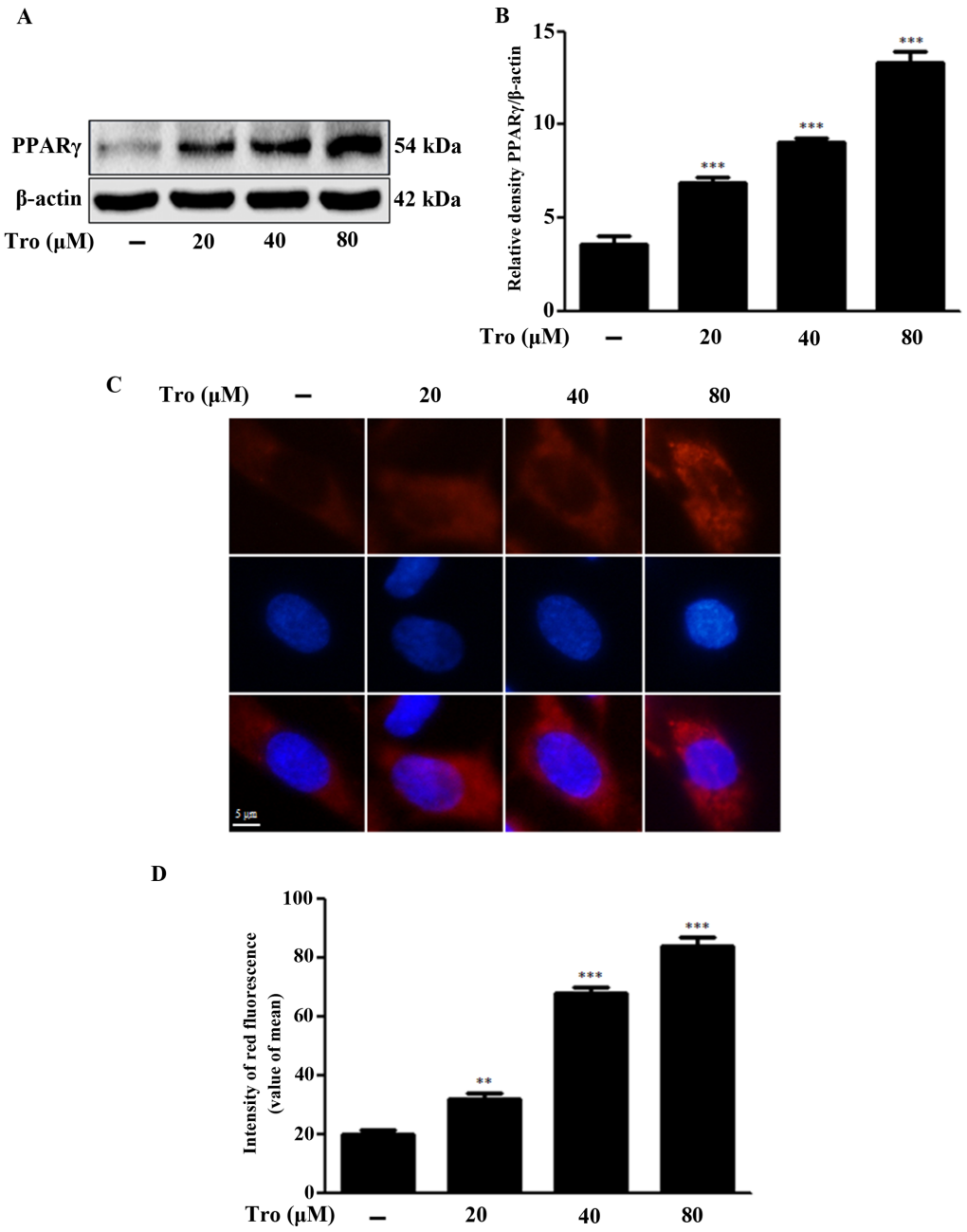

Figure 5. Troglitazone-stimulated PPARγ in neuronal cells. (A) Primary neuronal cells were treated with 20, 40 or 80 μM of troglitazone for 6 h. The treated cells were evaluated for PPARγ protein expression by western blot analysis. (B) Bar graph representing average PPARγ protein levels. Expression data were normalized to β-actin expression. Expression levels were evaluated by quantifying the protein bands, depicted by densitometric values beside the blot. Values represent the mean ± SD (n=5). ***P<0.001 vs. control. (C) SK-N-SH cells were treated with 20, 40, or 80 μM troglitazone for 6 h, then immunocytochemistry was employed to measure PPARγ protein expression levels. The cell nuclei were stained with DAPI (blue). (D) Bar graph representing the average red fluorescence intensity. Values represent the mean ± SD (n=5). **P<0.01, ***P<0.001 vs. control. Tro, troglitazone; PPARγ, peroxisome proliferator-activator receptor γ.

Although the function and mechanism of prion protein are still obscure, numerous studies have suggested that prior formation of prions are initiated by accumulation of PrPsc in the brain, analogous to amyloid-β in Alzheimer's disease (66-68).

Prior research has suggested that chemical drugs or plant extracts protect neurons during autophagy in neurodegenerative disease (69-73). The biological role of autophagy in neurodegenerative diseases, however, is debated. Nah *et al* (39) have suggested that abnormal autophagy could be induced by amyloid-β or accumulation of misfolded prion proteins in neuronal cells. In this study, we limited ourselves to experiments with PrP (106-126) in neuronal cells, not animal models. Accordingly, the prion peptide's autophagic effects have yet to be demonstrated *in vivo*, and further studies will be needed to discover whether prion peptide induces the neurotoxic effect that occurs during autophagy in mice models.

Most experiments were conducted using primary neuronal cells. In some experiments, SK-N-SH neuroblastoma cells were used (as described in the figure legends) as it proved difficult to observe fluorescent proteins in primary neuronal cells were, the cells was crushed and their shape destroyed, and as cells could no longer be propagated once they were

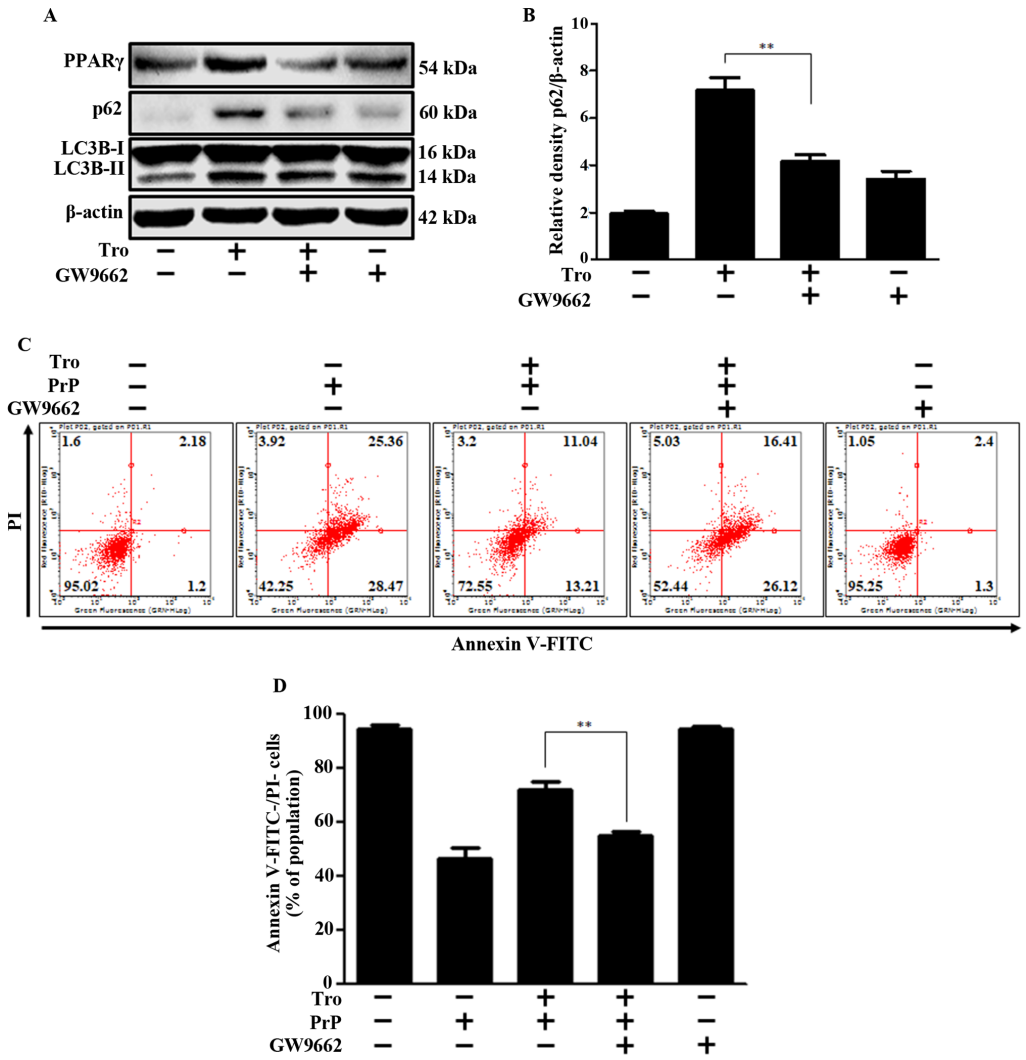

Figure 6. Troglitazone-induced inhibition of autophagy flux attenuated PrP (106-126)-induced neurotoxicity through PPARγ. (A) Primary neuronal cells were pretreated with PPARγ antagonist (GW9662) for 1 h and then exposed to 80 μM troglitazone for 6 h. The treated cells were evaluated for PPARγ, LC3B, and P62 protein expression by western blot analysis. β-actin was applied as a loading control. (B) Bar graph representing average p62 protein expression levels. Expression data were normalized to β-actin expression. Expression levels were evaluated by quantifying the protein bands, depicted by densitometric values beside the blot. Values represent the mean ± SD (n=5). **P<0.01. (C) SK-N-SH cells were pretreated with troglitazone in the absence or presence of GW9662 (1 h) and then exposed to 100 μM PrP (106-126) for 12 h. Cell viability was determined by an Annexin V/PI assay using FITC-Annexin V and PI, which combined with phosphatidylserine on the plasma membrane and nuclei during cellular apoptosis. Representative figures showing population of viable (Annexin V^-/PI^-), early apoptotic (Annexin V^+/PI^-), late apoptotic (Annexin V^+/PI^+) and necrotic (Annexin V^-/PI^+) cells. (D) Bar graph showing the averages of viable (Annexin V^-/PI^-) cells. Values represent the mean ± SD (n=10). **P<0.01. PrP, prion peptide (106-126); Tro, troglitazone; PPARγ, peroxisome proliferator-activator receptor γ.

terminally differentiated into mature neurons (74). SK-N-SH neuroblastoma cells, as the parental line of SH-SY5Y, have been widely used to characterize neuron-like behavior when investigating potential neuroprotective activity in *in vitro* models (74,75).

To obtain an understanding of their interplay, we examined the impact of troglitazone treatment on PrP-induced cell death, PPARγ, and autophagy flux in neuronal cells. This study revealed that PrP-mediated autophagic cell death could be prevented by troglitazone via neuronal PPARγ activation. Based on this study, regulating autophagy flux may be an effective means of mitigating the damage caused by prion diseases. Further studies could determine optimal strategies for the modulation of ROS for neurodegeneration treatment as ROS may be involved in both autophagy flux and prion diseases.

Acknowledgements

Not applicable.

Funding

This study was supported by a Korean Grant from the National Research Foundation (NRF) funded by the Ministry of Education (grant no. 2019R1A2B5B02069765) and 'Research Base Construction Fund Support Program' funded by Jeonbuk National University in 2020.

Availability of data and materials

The datasets used and/or analyzed during the current study are available from the corresponding author on reasonable request.

Authors' contributions

JHM, JMH and SYP designed and executed the study, analyzed the data and wrote the manuscript. JHM and SYP confirm the authenticity of all the raw data. All authors read and approved the final manuscript.

Ethics approval and consent to participate

This project received approval from the Institutional Review Board of Jeonbuk National University (approval no. CBNU-2019-00113).

Patient consent for publication

Not applicable.

Competing interests

The authors declare that they have no competing interests.

References

1. Peretz D, Williamson RA, Kaneko K, Vergara J, Leclerc E, Schmitt-Ulms G, Mehlhorn IR, Legname G, Wormald MR, Rudd PM, *et al*: Antibodies inhibit prion propagation and clear cell cultures of prion infectivity. Nature 412: 739-743, 2001.
2. Aguzzi A: Prion diseases of humans and farm animals: Epidemiology, genetics, and pathogenesis. J Neurochem 97: 1726-1739, 2006.
3. Scheckel C and Aguzzi A: Prions, prionoids and protein misfolding disorders. Nat Rev Genet 19: 405-418, 2018.
4. Aguzzi A and Heikenwalder M: Prion diseases: Cannibals and garbage piles. Nature 423: 127-129, 2003.
5. Forloni G, Chiesa R, Bugiani O, Salmona M and Tagliavini F: Review: PrP 106-126-25 years after. Neuropathol Appl Neurobiol 45: 430-440, 2019.
6. Fioriti L, Angeretti N, Colombo L, De Luigi A, Colombo A, Manzoni C, Morbin M, Tagliavini F, Salmona M, Chiesa R and Forloni G: Neurotoxic and gliotrophic activity of a synthetic peptide homologous to Gerstmann-Sträussler-Scheinker disease amyloid protein. J Neurosci 27: 1576-1583, 2007.
7. Fioriti L, Quaglio E, Massignan T, Colombo L, Stewart RS, Salmona M, Harris DA, Forloni G and Chiesa R: The neurotoxicity of prion protein (PrP) peptide 106-126 is independent of the expression level of PrP and is not mediated by abnormal PrP species. Mol Cell Neurosci 28: 165-176, 2005.
8. Villa A, Mark AE, Saracino GA, Cosentino U, Pitea D, Moro G and Salmona M: Conformational polymorphism of the PrP106-126 peptide in different environments: A molecular dynamics study. J Phys Chem B 110: 1423-1428, 2006.
9. Corsaro A, Thellung S, Villa V, Principe DR, Paludi D, Arena S, Millo E, Schettini D, Damonte G, Aceto A, *et al*: Prion protein fragment 106-126 induces a p38 MAP kinase-dependent apoptosis in SH-SY5Y neuroblastoma cells independently from the amyloid fibril formation. Ann NY Acad Sci 1010: 610-622, 2003.
10. Troglitazone. In: LiverTox: Clinical and Research Information on Drug-Induced Liver Injury. National Institute of Diabetes and Digestive and Kidney Diseases, Bethesda, MD, 2012.
11. Frias JP, Yu JG, Kruszynska YT and Olefsky JM: Metabolic effects of troglitazone therapy in type 2 diabetic, obese, and lean normal subjects. Diabetes care 23: 64-69, 2000.
12. Chandra V, Huang P, Hamuro Y, Raghuram S, Wang Y, Burris TP and Rastinejad F: Structure of the intact PPAR-gamma-RXR-nuclear receptor complex on DNA. Nature 456: 350-356, 2008.
13. Lehmann JM, Moore LB, Smith-Oliver TA, Wilkison WO, Willson TM and Kliewer SA: An antidiabetic thiazolidinedione is a high affinity ligand for peroxisome proliferator-activated receptor gamma (PPAR gamma). J Biol Chem 270: 12953-12956, 1995.
14. Olefsky JM and Saltiel AR: PPAR gamma and the treatment of insulin resistance. Trends Endocrinol Metab 11: 362-368, 2000.
15. Hong OY, Youn HJ, Jang HY, Jung SH, Noh EM, Chae HS, Jeong YJ, Kim W, Kim CH and Kim JS: Troglitazone inhibits matrix metalloproteinase-9 expression and invasion of breast cancer cell through a peroxisome proliferator-activated receptor γ-dependent mechanism. J Breast Cancer 21: 28-36, 2018.
16. Rosen ED and Spiegelman BM: PPARgamma: A nuclear regulator of metabolism, differentiation, and cell growth. J Biol Chem 276: 37731-37734, 2001.
17. Tontonoz P, Hu E and Spiegelman BM: Stimulation of adipogenesis in fibroblasts by PPAR gamma 2, a lipid-activated transcription factor. Cell 79: 1147-1156, 1994.
18. Jain MR, Giri SR, Trivedi C, Bhoi B, Rath A, Vanage G, Vyas P, Ranvir R and Patel PR: Saroglitazar, a novel PPARα/γ agonist with predominant PPARα activity, shows lipid-lowering and insulin-sensitizing effects in preclinical models. Pharmacol Res Perspect 3: e00136, 2015.
19. Certo M, Endo Y, Ohta K, Sakurada S, Bagetta G and Amantea D: Activation of RXR/PPARγ underlies neuroprotection by bexarotene in ischemic stroke. Pharmacol Res 102: 298-307, 2015.
20. Chiang MC, Cheng YC, Nicol CJ, Lin KH, Yen CH, Chen SJ and Huang RN: Rosiglitazone activation of PPARγ-dependent signaling is neuroprotective in mutant huntingtin expressing cells. Exp Cell Res 338: 183-193, 2015.
21. Lecca D, Nevin DK, Mulas G, Casu MA, Diana A, Rossi D, Sacchetti G, Fayne D and Carta AR: Neuroprotective and anti-inflammatory properties of a novel non-thiazolidinedione PPARγ agonist in vitro and in MPTP-treated mice. Neuroscience 302: 23-35, 2015.
22. Thouennon E, Cheng Y, Falahatian V, Cawley NX and Loh YP: Rosiglitazone-activated PPARγ induces neurotrophic factor-α1 transcription contributing to neuroprotection. J Neurochem 134: 463-470, 2015.
23. Jiang P and Mizushima N: Autophagy and human diseases. Cell Res 24: 69-79, 2014.
24. Lum JJ, Bauer DE, Kong M, Harris MH, Li C, Lindsten T and Thompson CB: Growth factor regulation of autophagy and cell survival in the absence of apoptosis. Cell 120: 237-248, 2005.
25. Mizushima N: Autophagy: Process and function. Genes Dev 21: 2861-2873, 2007.
26. Klionsky DJ, Abdelmohsen K, Abe A, Abedin MJ, Abeliovich H, Acevedo Arozena A, Adachi H, Adams CM, Adams PD, Adeli K, *et al*: Guidelines for the use and interpretation of assays for monitoring autophagy (3rd edition). Autophagy 12: 1-222, 2016.
27. Shintani T and Klionsky DJ: Autophagy in health and disease: A double-edged sword. Science 306: 990-995, 2004.
28. Bjørkøy G, Lamark T, Brech A, Outzen H, Perander M, Overvatn A, Stenmark H and Johansen T: p62/SQSTM1 forms protein aggregates degraded by autophagy and has a protective effect on huntingtin-induced cell death. J Cell Biol 171: 603-614, 2005.
29. Nakai A, Yamaguchi O, Takeda T, Higuchi Y, Hikoso S, Taniike M, Omiya S, Mizote I, Matsumura Y, Asahi M, *et al*: The role of autophagy in cardiomyocytes in the basal state and in response to hemodynamic stress. Nat Med 13: 619-624, 2007.
30. Su H, Li F, Ranek MJ, Wei N and Wang X: COP9 signalosome regulates autophagosome maturation. Circulation 124: 2117-2128, 2011.
31. Moon JH, Lee JH, Nazim UM, Lee YJ, Seol JW, Eo SK, Lee JH and Park SY: Human prion protein-induced autophagy flux governs neuron cell damage in primary neuron cells. Oncotarget 7: 29989-30002, 2016.
32. Beaudoin GM III, Lee SH, Singh D, Yuan Y, Ng YG, Reichardt LF and Arikkath J: Culturing pyramidal neurons from the early postnatal mouse hippocampus and cortex. Nat Protoc 7: 1741-1754, 2012.
33. Cho DH, Lee EJ, Kwon KJ, Shin CY, Song KH, Park JH, Jo I and Han SH: Troglitazone, a thiazolidinedione, decreases tau phosphorylation through the inhibition of cyclin-dependent kinase 5 activity in SH-SY5Y neuroblastoma cells and primary neurons. J Neurochem 126: 685-695, 2013.
34. Uryu S, Harada J, Hisamoto M and Oda T: Troglitazone inhibits both post-glutamate neurotoxicity and low-potassium-induced apoptosis in cerebellar granule neurons. Brain Res 924: 229-236, 2002.
35. Redmann M, Benavides GA, Berryhill TF, Wani WY, Ouyang X, Johnson MS, Ravi S, Barnes S, Darley-Usmar VM and Zhang J: Inhibition of autophagy with bafilomycin and chloroquine decreases mitochondrial quality and bioenergetic function in primary neurons. Redox Biol 11: 73-81, 2017.

36. Shacka JJ, Klocke BJ, Shibata M, Uchiyama Y, Datta G, Schmidt RE and Roth KA: Bafilomycin A1 inhibits chloroquine-induced death of cerebellar granule neurons. Mol Pharmacol 69: 1125-1136, 2006.
37. Wojtowicz AK, Szychowski KA and Kajta M: PPAR-γ agonist GW1929 but not antagonist GW9662 reduces TBBPA-induced neurotoxicity in primary neocortical cells. Neurotox Res 25: 311-322, 2014.
38. Martin HL, Mounsey RB, Mustafa S, Sathe K and Teismann P: Pharmacological manipulation of peroxisome proliferator-activated receptor γ (PPARγ) reveals a role for anti-oxidant protection in a model of Parkinson's disease. Exp Neurol 235: 528-538, 2012.
39. Nah J, Pyo JO, Jung S, Yoo SM, Kam TI, Chang J, Han J, Soo A An S, Onodera T and Jung YK: BECN1/Beclin 1 is recruited into lipid rafts by prion to activate autophagy in response to amyloid β 42. Autophagy 9: 2009-2021, 2013.
40. Saiki S, Sasazawa Y, Imamichi Y, Kawajiri S, Fujimaki T, Tanida I, Kobayashi H, Sato F, Sato S, Ishikawa K, *et al*: Caffeine induces apoptosis by enhancement of autophagy via PI3K/Akt/mTOR/p70S6K inhibition. Autophagy 7: 176-187, 2011.
41. Kumar D, Shankar S and Srivastava RK: Rottlerin-induced autophagy leads to the apoptosis in breast cancer stem cells: molecular mechanisms. Mol Cancer 12: 171, 2013.
42. Arsikin K, Kravic-Stevovic T, Jovanovic M, Ristic B, Tovilovic G, Zogovic N, Bumbasirevic V, Trajkovic V and Harhaji-Trajkovic L: Autophagy-dependent and -independent involvement of AMP-activated protein kinase in 6-hydroxydopamine toxicity to SH-SY5Y neuroblastoma cells. Biochim Biophys Acta 1822: 1826-1836, 2012.
43. Lee JH, Yoon YM, Han YS, Jung SK and Lee SH: Melatonin protects mesenchymal stem cells from autophagy-mediated death under ischaemic ER-stress conditions by increasing prion protein expression. Cell Prolif 52: e12545, 2019.
44. Jiang C, Ting AT and Seed B: PPAR-gamma agonists inhibit production of monocyte inflammatory cytokines. Nature 391: 82-86, 1998.
45. Ricote M, Li AC, Willson TM, Kelly CJ and Glass CK: The peroxisome proliferator-activated receptor-gamma is a negative regulator of macrophage activation. Nature 391: 79-82, 1998.
46. Combs CK, Johnson DE, Karlo JC, Cannady SB and Landreth GE: Inflammatory mechanisms in Alzheimer's disease: Inhibition of beta-amyloid-stimulated proinflammatory responses and neurotoxicity by PPARgamma agonists. J Neurosci 20: 558-567, 2000.
47. Beheshti F, Hosseini M, Hashemzehi M, Soukhtanloo M, Khazaei M and Shafei MN: The effects of PPAR-γ agonist pioglitazone on hippocampal cytokines, brain-derived neurotrophic factor, memory impairment, and oxidative stress status in lipopolysaccharide-treated rats. Iran J Basic Med Sci 22: 940-948, 2019.
48. Zhang H, Gong M and Luo X: Methoxytetrahydro-2H-pyran-2-yl) methyl benzoate inhibits spinal cord injury in the rat model via PPAR-γ/PI3K/p-Akt activation. Environ Toxicol 35: 714-721, 2020.
49. de Brito TV, Júnior GJD, da Cruz Júnior JS, Silva RO, da Silva Monteiro CE, Franco AX, Vasconcelos DFP, de Oliveira JS, da Silva Costa DV, Carneiro TB, *et al*: Gabapentin attenuates intestinal inflammation: Role of PPAR-gamma receptor. Eur J Pharmacol 873: 172974, 2020.
50. Khasabova IA, Khasabov SG, Olson JK, Uhelski ML, Kim AH, Albino-Ramírez AM, Wagner CL, Seybold VS and Simone DA: Pioglitazone, a PPARγ agonist, reduces cisplatin-evoked neuropathic pain by protecting against oxidative stress. Pain 160: 688-701, 2019.
51. Aoun P, Watson DG and Simpkins JW: Neuroprotective effects of PPARgamma agonists against oxidative insults in HT-22 cells. Eur J Pharmacol 472: 65-71, 2003.
52. Jodeiri Farshbaf M, Forouzanfar M, Ghaedi K, Kiani-Esfahani A, Peymani M, Shoaraye Nejati A, Izadi T, Karbalaie K, Noorbakhshnia M, Rahgozar S, *et al*: Nurr1 and PPARγ protect PC12 cells against MPP(+) toxicity: Involvement of selective genes, anti-inflammatory, ROS generation, and antimitochondrial impairment. Mol Cell Biochem 420: 29-42, 2016.
53. Mahmood DFD, Jguirim-Souissi I, Khadija EH, Blondeau N, Diderot V, Amrani S, Slimane MN, Syrovets T, Simmet T and Rouis M: Peroxisome proliferator-activated receptor gamma induces apoptosis and inhibits autophagy of human monocyte-derived macrophages via induction of cathepsin L: Potential role in atherosclerosis. J Biol Chem 286: 28858-28866, 2011.
54. Yao J, Zheng K and Zhang X: Rosiglitazone exerts neuroprotective effects via the suppression of neuronal autophagy and apoptosis in the cortex following traumatic brain injury. Mol Med Rep 12: 6591-6597, 2015.
55. Gao N, Yao X, Jiang L, Yang L, Qiu T, Wang Z, Pei P, Yang G, Liu X and Sun X: Taurine improves low-level inorganic arsenic-induced insulin resistance by activating PPARγ-mTORC2 signalling and inhibiting hepatic autophagy. J Cell Physiol 234: 5143-5152, 2019.
56. Hu C, Chen C, Chen J, Xiao K, Wang J, Shi Q, Ma Y, Gao LP, Wu YZ, Liu L, *et al*: The low levels of nerve growth factor and its upstream regulatory kinases in prion infection is reversed by resveratrol. Neurosci Res 162: 52-62, 2021.
57. Jeong JK, Moon MH, Bae BC, Lee YJ, Seol JW, Kang HS, Kim JS, Kang SJ and Park SY: Autophagy induced by resveratrol prevents human prion protein-mediated neurotoxicity. Neurosci Res 73: 99-105, 2012.
58. Tagliavini F, Forloni G, D'Ursi P, Bugiani O and Salmona M: Studies on peptide fragments of prion proteins. Adv Protein Chem 57: 171-201, 2001.
59. Ilitchev AI, Giammona MJ, Olivas C, Claud SL, Lazar Cantrell KL, Wu C, Buratto SK and Bowers MT: Hetero-oligomeric amyloid assembly and mechanism: Prion fragment PrP(106-126) catalyzes the islet amyloid polypeptide β-hairpin. J Am Chem Soc 140: 9685-9695, 2018.
60. Singh N, Gu Y, Bose S, Kalepu S, Mishra RS and Verghese S: Prion peptide 106-126 as a model for prion replication and neurotoxicity. Front Biosci 7: a60-a71, 2002.
61. Herrmann US, Sonati T, Falsig J, Reimann RR, Dametto P, O'Connor T, Li B, Lau A, Hornemann S, Sorce S, *et al*: Prion infections and anti-PrP antibodies trigger converging neurotoxic pathways. PLoS Pathog 11: e1004662, 2015.
62. Tremblay P, Ball HL, Kaneko K, Groth D, Hegde RS, Cohen FE, DeArmond SJ, Prusiner SB and Safar JG: Mutant PrPSc conformers induced by a synthetic peptide and several prion strains. J Virol 78: 2088-2099, 2004.
63. Zhu C, Herrmann US, Li B, Abakumova I, Moos R, Schwarz P, Rushing EJ, Colonna M and Aguzzi A: Triggering receptor expressed on myeloid cells-2 is involved in prion-induced microglial activation but does not contribute to prion pathogenesis in mouse brains. Neurobiol Aging 36: 1994-2003, 2015.
64. Giaccone G and Moda F: PMCA applications for prion detection in peripheral tissues of patients with variant creutzfeldt-jakob disease. Biomolecules 10: 405, 2020.
65. Haley NJ and Hoover EA: Chronic wasting disease of cervids: Current knowledge and future perspectives. Annu Rev Anim Biosci 3: 305-325, 2015.
66. Kaufman SK and Diamond MI: Prion-like propagation of protein aggregation and related therapeutic strategies. Neurotherapeutics 10: 371-382, 2013.
67. Aguzzi A and Calella AM: Prions: Protein aggregation and infectious diseases. Physiol Rev 89: 1105-1152, 2009.
68. Zhu C, Li B, Frontzek K, Liu Y and Aguzzi A: SARM1 deficiency up-regulates XAF1, promotes neuronal apoptosis, and accelerates prion disease. J Exp Med 216: 743-756, 2019.
69. Jeong JK and Park SY: Melatonin regulates the autophagic flux via activation of alpha-7 nicotinic acetylcholine receptors. J Pineal Res 59: 24-37, 2015.
70. Damme M, Suntio T, Saftig P and Eskelinen EL: Autophagy in neuronal cells: General principles and physiological and pathological functions. Acta Neuropathol 129: 337-362, 2015.
71. Lee JH, Jeong JK and Park SY: Sulforaphane-induced autophagy flux prevents prion protein-mediated neurotoxicity through AMPK pathway. Neuroscience 278: 31-39, 2014.
72. Ciechanover A and Kwon YT: Degradation of misfolded proteins in neurodegenerative diseases: Therapeutic targets and strategies. Exp Mol Med 47: e147, 2015.
73. Nakagaki T, Satoh K, Ishibashi D, Fuse T, Sano K, Kamatari YO, Kuwata K, Shigematsu K, Iwamaru Y, Takenouchi T, *et al*: FK506 reduces abnormal prion protein through the activation of autolysosomal degradation and prolongs survival in prion-infected mice. Autophagy 9: 1386-1394, 2013.
74. Kovalevich J and Langford D: Considerations for the use of SH-SY5Y neuroblastoma cells in neurobiology. Methods Mol Biol 1078: 9-21, 2013.
75. Forster JI, Köglsberger S, Trefois C, Boyd O, Baumuratov AS, Buck L, Balling R and Antony PM: Characterization of differentiated SH-SY5Y as neuronal screening model reveals increased oxidative vulnerability. J Biomol Screen 21: 496-509, 2016.